Descriptor Sliding Mode Observer Based Fault Tolerant Control for Nuclear Power Plant with Actuator and Sensor Faults

Piyush V. Surjagade[a,*], Jiamei Deng[a,*], S. R. Shimjith[b], A. John Arul[c]

[a] *School of Built Environment, Engineering and Computing, Leeds Beckett University, Leeds, LS6 3QR, United Kingdom.*
[b] *Reactor Control Division, Bhabha Atomic Research Centre, Mumbai, 400 085, India and Homi Bhabha National Institute, Mumbai, 400 094, India.*
[c] *Probabilistic Safety, Reactor Shielding and Nuclear Data Section, Indira Gandhi Centre for Atomic Research, Kalpakkam, 603 102, India.*

Abstract

In sophisticated and complex system such as nuclear power plant, fault estimation and fault tolerant control always play an important role in maintaining the system stability and assuring satisfactory and safe operation. Thus, in this work a fault estimation and fault tolerant control scheme based on sliding mode theory is proposed for a pressurized water reactor type nuclear power plant considering simultaneous actuator and sensor faults. First, using descriptor sliding mode observer approach, an accurate estimation of the system states and sensor fault vector have been obtained simultaneously. Then, based on the estimated information, an integral type sliding mode control scheme is proposed to stabilize the resulting faulty system. With the help of Lyapunov stability theory, reachabilities of the proposed sliding mode surfaces are shown in both the state estimation space and the error estimation space, simultaneously. Finally, the efficacy of the proposed control scheme is shown by applying it to a nuclear power plant.

Key words: Fault tolerant control, fault estimation, sliding mode control,

*Corresponding authors
Email addresses: p.surjagade@leedsbeckett.ac.uk (Piyush V. Surjagade), j.deng@leedsbeckett.ac.uk (Jiamei Deng), srshim@barc.gov.in (S. R. Shimjith), arul@igcar.gov.in (A. John Arul)

descriptor system, large-scale system, nuclear power plant

1. Introduction

A facility designed to convert nuclear energy into electricity is called a Nuclear Power Plant (NPP). An NPP is a complex nonlinear system, where system parameters vary with fuel burn-up, internal reactivity feedbacks, and with the change in the power levels and operating conditions. These variations in system parameters along with other system uncertainties such as unmodeled dynamics and external disturbances, make NPP control a very difficult task. Thus, a simple and high precision control strategy, which guarantees satisfactory performance in the presence of these uncertainties, is always preferable for an NPP.

In the past decades, different types of robust and adaptive control strategies have been proposed for NPPs to achieve the desired dynamic performance. Among different robust and adaptive control design techniques, Sliding Mode Control (SMC) technique has been extensively studied and widely applied to the control of NPPs [1, 2, 3, 4, 5, 6] because of its inherent robustness against matched uncertainties, simple structure, ease of implementation, and capability to effectively control both linear as well as nonlinear systems [7]. *Vajpayee et al.* [1] designed a robust subspace predictive control for a Pressurized Water Reactor (PWR) by combing a subspace-based predictive control with an integral SMC. *Desai et al.* [2] and *Patre et al.* [3] proposed an integral SMC and a fuzzy SMC for spatial power control of advanced heavy water reactor, respectively. In [4], a fractional-order SMC has been proposed for output power control of a research reactor based on non-linear reduced-order fractional-order model. A hybrid optimal controller combining linear quadratic Gaussian/loop transfer recovery and integral SMC for a PWR operating in the load-following mode has been proposed in [5]. Mostafavi and Ansarifar [6] proposed an observer-based dynamic SMC using Lyapunov-approach for level control of pressurizer in PWR type NPP.

Almost all the above mentioned approaches have been developed under the

assumption that there is no presence of faults in the actuators and/or sensors. However, during normal operation of NPPs, various malfunctions and imperfect behaviour are inevitable, which resulted from the unexpected variations in external surroundings and sudden change in signals. Such kinds of phenomenons are categorized as faults. Faults are further classified as actuator faults, process or plant faults, and sensor faults depending on their location. In sophisticated and complex systems such as NPP, faults may lead to loss of effectiveness or sometimes total failure of the overall plant, which may further lead to catastrophic events, thereby causing both economic losses as well as human casualties. Thus, in order to improve safety and reliability of NPPs and to reduce economic losses, it is necessary to design the control system which is capable of tolerating potential faults while maintaining acceptable performance. Such type of control system is known as fault-tolerant control (FTC) system. Over the past few decades, due to increasing demand for higher safety and reliability standards in the NPPs, the development of Fault Estimation (FE) and FTC systems has received considerable attention. In general, FTC schemes involve two steps: first step is the fault diagnosis that is, detection, estimation, or reconstruction of faults [8, 9, 10, 11, 12] and second step is the controller design based on the fault information to eliminate the effects of faults or attenuate them within an acceptable limit [13, 14, 15, 16, 17].

Over the past few decades, various fault detection/estimation and FTC techniques have been developed for NPPs. For the safe and stable operation of NPPs, actuators as driving elements and sensors as information transmission elements play an important role. Thus, accommodation of actuator and sensor faults have received considerable attention among the researchers. In [18], authors proposed the use of Sliding Mode Observer (SMO) for robust fault detection and isolation in nuclear reactor system as well as in steam generator and pressurizer system in the presence of uncertainties and noise. *Dong* [19] proposed a boolean network model in a linear representation for describing the fault propagation among sensors for a nuclear steam supply system based on a modular high temperature gas-cooled reactor. *Gautam et al.* [9] proposed a robust

fault detection algorithm using extended Kalman filter and Kullback-Leibler divergence for non-linear PWR-NPP subject to parametric additive time-varying incipient fault in the measurements. Authors consider the problem of both single and simultaneous multiple sensors incipient fault detection and isolation. In [20], recurrent neuro-fuzzy systems is adopted, in which a fuzzification module is linked to a neural network interface module, for fault detection and isolation in PWR. In [21], authors proposed an FTC system in the presence of actuator failures using fault detection and isolation approach while keeping the system reachable or controllable. *Hatami et al.* [13, 14] proposed adaptive neuro-fuzzy FTCs based on emotional learning for load following mode of operation in NPP. Authors used extended Kalman filter and recursive least square method to estimate the parameters of the system. In [11] and [12], authors proposed a multi-scale Principal Component Analysis (PCA) by integrating wavelet with PCA and a hybrid multi-scale data reconciliation scheme by combining data reconciliation with the wavelet transform, respectively for detection and isolation of sensor and process faults in advanced heavy water reactor. *Yu et al.* [22] proposed a corrected reconstruction algorithm to improve the accuracy of conventional PCA techniques while reconstructing multi-sensor faults and a cyclic PCA monitoring model to detect multi-sensor failures. *Khentout et al.* [15] presented fault monitoring and accommodation of the heat exchanger parameters of Triga-Mark II nuclear research reactor using model based analytical redundancy. *Wang et al.* [17] proposed a fuzzy fault accommodation method for a small pressurized water reactor under control rod driven mechanism struck faults and feed water valve stuck faults. In [16], authors proposed an FTC for a nuclear steam generator in the presence of sensor biases. The bias present in the measurements is modeled as a time varying parameter and estimated using a suitably modified version of RNK based state and parameter estimator approach and then the controller is designed based on the corrected measurements. Almost all the above fault detection/estimation and FTC schemes have either focused only on sensor faults or only on actuator faults or based on the assumption that only either an actuator or a sensor fault present at a given in-

stant of time. However, the simultaneous consideration of actuator and sensor faults has yet to be investigated.

Motivated by the aforementioned problems, in this paper, an observer-based FTC scheme is designed for PWR-NPP considering simultaneous actuator and sensor faults. To design the proposed control scheme, the original system is augmented into a descriptor system, in which system states and sensor faults form a new state vector of the augmented system. First, the SMO is designed for the augmented system to estimate system states and sensor faults simultaneously. The proposed observer is insensitive towards parameter variations and external disturbances, has high accuracy, and gives finite time convergence compared to conventional observers. With the help of Linear Matrix Inequalities (LMIs), a sufficient condition is given to ensure asymptotic stability of the overall closed-loop system consisting of both state observer and estimation error system. Then, based on the estimated information, an integral SMC based FTC scheme is designed to stabilize the closed-loop faulty system. With the help of Lyapunov stability theory, it is shown that the proposed control law guarantees that the trajectories of the closed-loop system in both error estimation and state estimation spaces can be kept onto the corresponding switching surfaces. Finally, the effectiveness of the proposed control scheme is shown with the help of simulation results by applying it to a PWR-NPP. The major contributions of the proposed work are summarized as follows:

- The overall problem of active FTC is considered i.e., detection of faults as well as elimination/attenuation of faults.
- The proposed control scheme considers the effect of simultaneous actuator and sensor faults.
- A sufficient condition is derived using LMIs to ensure overall stability of the closed-loop system.

The rest of the paper is organized as follows: Section 2 formulates the control problem. Section 3 explains the design procedure of the proposed fault tolerant

control scheme. Application of the proposed control scheme to PWR-NPP is presented in Section 4. Finally, conclusions are drawn in Section 5 indicating main contributions.

2. Problem Formulation

Let us consider an uncertain linear continuous-time system represented as

$$\dot{x}(t) = Ax(t) + B(u(t) + f_a(t)) \tag{1a}$$

$$y(t) = Cx(t) + f_s(t) \tag{1b}$$

where $x(t) \in \mathbb{R}^n$ is the system state vector, $u(t) \in \mathbb{R}^m$ is the control input vector, $y(t) \in \mathbb{R}^p$ is the output measurement vector, $f_a(t) \in \mathbb{R}^m$ represents the actuator fault vector, and $f_s(t) \in \mathbb{R}^p$ represents the sensor fault vector. $A \in \mathbb{R}^{n\times n}$, $B \in \mathbb{R}^{n\times m}$, and $C \in \mathbb{R}^{p\times n}$ are the system matrices.

For system (1) following assumptions are made:

Assumption 1. *The actuator fault $f_a(t)$ and the sensor fault $f_s(t)$ are unknown but bounded and satisfy the following conditions:*

$$\|f_a(t)\| \leq f_a^* \quad \textit{and} \quad \|f_s(t)\| \leq f_s^* \tag{2}$$

where f_a^* and f_s^* are known positive constants.

Assumption 2. *Matrix pair (A, B) is controllable and matrix B has full column rank.*

Assumption 3. *Matrix pair (A, C) is observable and matrix C has full row rank.*

For system (1), control aim is to develop an effective FE and FTC strategy such that the asymptotic estimation of the state vector and sensor fault vector can be obtained simultaneously, and to guarantee the resulting closed-loop system to be stable in the presence of actuator and sensor faults.

3. Proposed Approach

In order to obtain the accurate estimation of system states and sensor faults, the system (1) is augmented as

$$E_a\dot{x}_a(t) = A_a x_a(t) + B_a u(t) + H_a f(t) \tag{3a}$$

$$y(t) = C_a x_a(t) \tag{3b}$$

where

$$x_a(t) = \begin{bmatrix} x(t) \\ f_s(t) \end{bmatrix},\ f(t) = \begin{bmatrix} f_a(t) \\ f_s(t) \end{bmatrix},$$

$$A_a = \begin{bmatrix} A & 0_{n\times p} \\ 0_{p\times n} & -I_p \end{bmatrix},\ B_a = \begin{bmatrix} B \\ 0_{p\times m} \end{bmatrix},\ C_a = \begin{bmatrix} C\ I_p \end{bmatrix},$$

$$H_a = \begin{bmatrix} B & 0_{n\times p} \\ 0_{p\times m} & I_p \end{bmatrix},\ E_a = \begin{bmatrix} I_n & 0_{n\times p} \\ 0_{p\times n} & 0_{p\times p} \end{bmatrix}.$$

System (3) is a descriptor system model where the state vector $x(t)$ and sensor fault vector $f_s(t)$ are considered as a descriptor system state vector $x_a(t)$. The superiority of this transformation is that if an effective state observer is designed for the descriptor system (3), then the original states and sensor faults could be estimated simultaneously. In this work, to obtain the estimates of descriptor state vector, a SMO is proposed.

Remark1. In (1), it is assumed that the actuator fault vector $f_a(t)$ satisfies the matching condition (space span by the input distribution matrix). Thus, its effect can be easily overcome by the SMC as the SMC is insensitive towards matched type of faults. Therefore, in this work, in descriptor system model (3) only the sensor fault vector is augmented with the state vector.

Remark2. The effect of mismatched types of actuator faults can be minimized by estimating its value and then by designing a feedforward control based on the estimated information. To estimate mismatched actuator fault vector, the state vector of the descriptor system model (3) needs to be augmented with mismatched actuator fault vector along with the the system state and sensor faults vector.

3.1. Sliding Mode Observer Design

This section focuses on the design of SMO to obtain the estimates of the system state vector and sensor fault vector, simultaneously. The following lemma is significant and crucial for the subsequent development of the observer design.

Lemma 1. *[23] There always exist a matrix $L_D \in \mathbb{R}^{(n+p)\times p}$ such that the matrix $S = (E_a + L_D C_a)$ is nonsingular. Furthermore, it holds that $C_a S^{-1} L_D = I_p$ and $A_a S^{-1} L_D = -R$, where $R = \begin{bmatrix} 0_{p\times n} & I_p \end{bmatrix}^\top$.*

The proof of Lemma 1 is given in Appendix A.

Based on the above lemma, the SMO for descriptor system (3) is designed as [23]

$$S\dot{z}(t) = (A_a - L_p C_a)z(t) + B_a u(t) - Ry(t) + L_s u_s(t) \tag{4a}$$

$$\hat{x}_a(t) = z(t) + S^{-1} L_D y(t), \tag{4b}$$

where $z(t) = \begin{bmatrix} z_x(t)^\top & z_{f_s}(t)^\top \end{bmatrix}^\top$ is the intermediate state variable, $\hat{x}_a(t) = \begin{bmatrix} \hat{x}(t)^\top & \hat{f}_s(t)^\top \end{bmatrix}^\top$ is the estimation of $x_a(t)$, and $u_s(t)$ is the discontinuous injection added to eliminate the effect of disturbance. L_p and L_s are the proportional and discontinuous observer gains and are designed to satisfy $L_p = SP^{-1}C_a^\top$ and $L_s = SP^{-1}C_a^\top U^\top = H_a$, respectively, where $P \in \mathbb{R}^{(n+p)\times(n+p)} > 0$ and $U \in \mathbb{R}^{(m+p)\times p}$ are the matrices to be designed. Let matrix L_D is defined as $L_D = \begin{bmatrix} 0_{p\times n} & W \end{bmatrix}^\top$, where $W \in \mathbb{R}^{p\times p}$ and is selected as $W = \mathrm{diag}(w_1,\ w_2,\ \ldots,\ w_p)$ with $w_i > 0$.

In the following, the error system dynamics are derived from the augmented

system (3) and the observer (4). From (4), we have

$$\begin{aligned}
S\dot{\hat{x}}_a(t) &= S\dot{z}(t) + L_D\dot{y}(t) \\
&= (A_a - L_pC_a)z(t) + B_au(t) - Ry(t) \\
&\quad + L_su_s(t) + L_D\dot{y}(t) \\
&= (A_a - L_pC_a)(\hat{x}_a(t) - S^{-1}L_Dy(t)) + B_au(t) \\
&\quad - Ry(t) + L_su_s(t) + L_D\dot{y}(t) \\
&= (A_a - L_pC_a)\hat{x}_a(t) - A_aS^{-1}L_Dy(t) \\
&\quad + L_pC_aS^{-1}L_Dy(t) + B_au(t) \\
&\quad - Ry(t) + L_su_s(t) + L_D\dot{y}(t). \qquad (5)
\end{aligned}$$

Using Lemma 1, (5) can be simplified to

$$\begin{aligned}
S\dot{\hat{x}}_a(t) &= (A_a - L_pC_a)\hat{x}_a(t) + Ry(t) + L_py(t) \\
&\quad + B_au(t) - Ry(t) + L_su_s(t) + L_D\dot{y}(t) \\
&= (A_a - L_pC_a)\hat{x}_a(t) + L_py(t) \\
&\quad + B_au(t) + L_su_s(t) + L_D\dot{y}(t). \qquad (6)
\end{aligned}$$

On the other hand, adding $L_D\dot{y}(t)$ to the both side of system (3a), we get

$$\begin{aligned}
S\dot{x}_a(t) &= A_ax_a(t) + B_au(t) + H_af(t) + L_D\dot{y}(t) \\
&= (A_a - L_pC_a)x_a(t) + B_au(t) + H_af(t) \\
&\quad + L_py(t) + L_D\dot{y}(t). \qquad (7)
\end{aligned}$$

Now, defining the estimation error as $e(t) = \hat{x}_a(t) - x_a(t)$, the estimation error dynamics is obtained as

$$\dot{e}(t) = S^{-1}\Big[(A_a - L_pC_a)e(t) + L_su_s(t) - H_af(t)\Big]. \qquad (8)$$

The state variable of observer dynamics (6) is the augmented vector *i.e.*, $\hat{x}_a(t) = \left[\hat{x}(t)^\top \ \hat{f}_s(t)^\top\right]^\top$ which does not facilitate the stability analysis of the system (6). Therefore, in the following, the observer dynamics (6) has been decomposed into an estimated state vector dynamics $\dot{\hat{x}}(t)$. The observer dynamics

(6) can be rewritten as

$$E_a\dot{\hat{x}}_a(t) + L_D C_a \dot{\hat{x}}_a(t) = (A_a - L_p C_a)\hat{x}_a(t) + L_p y(t) + B_a u(t) + L_s u_s(t) + L_D \dot{y}(t) \tag{9}$$

or

$$E_a\dot{\hat{x}}_a(t) = A_a\hat{x}_a(t) - L_p C_a e(t) + B_a u(t) + L_s u_s(t) - L_D C_a \dot{e}(t). \tag{10}$$

Recalling $\hat{x}_a(t) = \begin{bmatrix}\hat{x}(t)^\top & \hat{f}_s(t)^\top\end{bmatrix}^\top \in \mathbb{R}^{(n+p)}$ and $L_s = H_a$, and decomposing matrices $L_D = \begin{bmatrix}L_{D_1}^\top & L_{D_2}^\top\end{bmatrix}^\top \in \mathbb{R}^{(n+p)\times p}$, $L_p = \begin{bmatrix}L_{p_1}^\top & L_{p2}^\top\end{bmatrix}^\top \in \mathbb{R}^{(n+p)\times p}$, $L_s = \begin{bmatrix}L_{s_1}^\top & L_{s_2}^\top\end{bmatrix}^\top \in \mathbb{R}^{(n+p)\times(m+p)}$, and $u_s(t) = \begin{bmatrix}u_{s_1}(t)^\top & u_{s_2}(t)^\top\end{bmatrix}^\top \in \mathbb{R}^{(m+p)}$, (10) can be decomposed as

$$\dot{\hat{x}}(t) = A\hat{x}(t) - L_{p_1} C_a e(t) + Bu(t) + L_{s_1} u_{s_1}(t) - L_{D_1} C_a \dot{e}(t). \tag{11}$$

It is easy to verify that $L_{s_1} = [B \;\; 0_{n\times p}] \in \mathbb{R}^{n\times(m+p)}$, $L_{D_1} = 0_{n\times p} \in \mathbb{R}^{n\times p}$, and $L_{D_2} = W \in \mathbb{R}^{p\times p}$. Thus, (11) is reduces to

$$\dot{\hat{x}}(t) = A\hat{x}(t) - L_{p_1} C_a e(t) + Bu(t) + Bu_{s_1}(t). \tag{12}$$

3.2. Observer Based Sliding Mode Control Design

In this section, the discontinuous observer input $u_s(t)$ and the control input $u(t)$ have been designed to stabilize the systems (8) and (12). As the system is affected by actuator as well as sensor faults, in this work, both the inputs are designed using robust sliding mode theory.

First, the discontinuous observer input $u_s(t)$ is designed. For the design of $u_s(t)$, the switching surface is defined in term of estimation error $e(t)$ as

$$\sigma_e(t) = H_a^\top S^{-\top} P e(t), \tag{13}$$

where $\sigma_e(t) \in \mathbb{R}^{m+p}$, and the designed Lyapunov matrix $P > 0$ is to be constructed such that it satisfies the following constraint

$$H_a^\top S^{-\top} P = U C_a, \tag{14}$$

where $U \in \mathbb{R}^{(m+p)\times p}$ is the parameter matrix to be determined.

Note that, in (13), $e(t)$ is unknown and thus, $\sigma_e(t)$ is unavailable. However, output error variable $e_y(t) = C_a e(t) = C_a\hat{x}_a(t) - C_a x_a(t)$ is available since, both $C_a\hat{x}_a(t)$ and $C_a x_a(t)$ are known. Therefore, by introducing constraint (14), the switching surface

$$\sigma_e(t) = H_a^\top S^{-\top} P e(t) = U C_a e(t) \tag{15}$$

is available for the controller design. The discontinuous observer input $u_s(t)$ is designed as

$$u_s(t) = -\mu_o \ \text{sign}(\sigma_e(t)), \tag{16}$$

where $\mu_o \geq (f_a^* + f_s^* + \eta)$ is the discontinuous gain and sign(.) is the standard signum function. $\eta > 0$ is the parameter to be designed.

Second, the control input $u(t)$ is designed as consisting of two parts, a continuous part, and a discontinuous part, and it is constructed using the estimated state vector $\hat{x}(t)$ as

$$u(t) = \underbrace{-K_x\hat{x}(t) - K_r r(t)}_{u_c(t)} \underbrace{-\mu_{c_1}\sigma_{\hat{x}}(t) - \mu_{c_2}\text{sign}(\sigma_{\hat{x}}(t))}_{u_d(t)}, \tag{17}$$

where $u_c(t)$ is the continuous nominal control, $u_d(t)$ is the discontinuous control, K_x is the state feedback control gain responsible for the performance of the nominal system which can be designed by any state feedback control design technique, K_r is the feed-forward control gain introduced to track the desired reference signal $r(t)$, and $\mu_{c_1} > 0$ and $\mu_{c_2} > 0$ are the discontinuous control gains which are designed using exponential reaching law. In (17), the switching surface $\sigma_{\hat{x}}(t)$ is designed as

$$\sigma_{\hat{x}}(t) = G\Big[\hat{x}(t) - \hat{x}(0) - \int_0^t \Big(A\hat{x}(\tau) - BK_x\hat{x}(\tau) - BK_r r(\tau)\Big)d\tau\Big], \tag{18}$$

where $G \in \mathbb{R}^{m\times n}$ is the projection matrix. Here, G is selected as left pseudo-inverse of input distribution matrix *i.e.*, $G = (B^\top B)^{-1}B^\top$ such that GB is invertible. The term $-G\hat{x}(0)$ ensures that $\sigma_{\hat{x}}(0) = 0$, thereby eliminating the reaching phase.

The control action required to maintain the sliding motion is known as equivalent control, and it is obtained by setting $\dot{\sigma}_{\hat{x}}(t) = 0$. Using (18) and (12), the equivalent control is computed as

$$u_{eq}(t) = -K_x\hat{x}(t) - K_r r(t) - u_{s_1}(t) + (GB)^{-1}GL_{p_1}C_a e(t). \tag{19}$$

Now, substituting (19) in (12), the sliding mode dynamics in the state estimation space is given by

$$\begin{aligned}\dot{\hat{x}}(t) = (A - BK_x)\hat{x}(t) - BK_r r(t)\\ +\Big[B(GB)^{-1}G - I\Big]L_{p_1}C_a e(t).\end{aligned} \tag{20}$$

As a result, the sliding mode dynamics (20) and the error dynamics (8) form the overall closed loop system as

$$\begin{aligned}\dot{\hat{x}}(t) &= (A - BK_x)\hat{x}(t) - BK_r r(t)\\ &\quad +\Big[B(GB)^{-1}G - I\Big]L_{p_1}C_a e(t), &\text{(21a)}\\ \dot{e}(t) &= S^{-1}\Big[(A_a - L_pC_a)e(t) + L_s u_s(t) - H_a f(t)\Big]. &\text{(21b)}\end{aligned}$$

3.3. Stability Analysis of Closed-Loop System

In this section, sufficient conditions for asymptotic stability of the closed-loop system (21) have been derived.

Theorem 1. *If there exist positive definite matrices $Q \in \mathbb{R}^{n\times n}$ and $P \in \mathbb{R}^{(n+p)\times(n+p)}$, and $U \in \mathbb{R}^{(m+p)\times p}$ such that the following symmetric matrix constraints*

$$\Gamma = \begin{bmatrix}\Gamma_{11} & \Gamma_{12} & \Gamma_{13}\\ \star & \Gamma_{22} & \Gamma_{23}\\ \star & \star & \Gamma_{33}\end{bmatrix} < 0, \tag{22}$$

and

$$H_a^\top S^{-\top} P - UC_a = 0, \tag{23}$$

hold, where

$$\begin{aligned}
\Gamma_{11} &= Q(A - BK_x) + (A - BK_x)^\top Q, \\
\Gamma_{12} &= Q\Big[B(GB)^{-1}G - I\Big]L_{p_1}C_a, \\
\Gamma_{13} &= -QBK_r, \\
\Gamma_{22} &= PS^{-1}(A_a - L_pC_a) + (A_a - L_pC_a)^\top S^{-T}P, \\
\Gamma_{23} &= 0, \\
\Gamma_{33} &= 0,
\end{aligned}$$

then, under the sliding mode observer input $u_s(t)$ defined in (18), the overall closed-loop system (21) is asymptotically stable.

Proof. *Consider the Lyapunov function*

$$V(t) = V_{\hat{x}}(t) + V_e(t) \tag{24}$$

where

$$\begin{aligned}
V_{\hat{x}}(t) &= \hat{x}(t)^\top Q\hat{x}(t), \\
V_e(t) &= e(t)^\top Pe(t).
\end{aligned}$$

220 *Taking the weak infinitesimal operator ($\mathcal{L}$) along the trajectories of system (21), we get*

$$\begin{aligned}
\mathcal{L}V_{\hat{x}}(t) &= 2\hat{x}(t)^\top Q\Big\{(A - BK_x)\hat{x}(t) - BK_r r(t) \\
&\quad + \Big[B(GB)^{-1}G - I\Big]L_{p_1}C_a e(t)\Big\} \\
&= \hat{x}(t)^\top \Big[Q(A - BK_x) + (A - BK_x)^\top Q\Big]\hat{x}(t) \\
&\quad + 2\hat{x}(t)^\top Q\Big[B(GB)^{-1}G - I\Big]L_{p_1}C_a e(t) \\
&\quad - 2\hat{x}(t)^\top QBK_r r(t),
\end{aligned} \tag{25}$$

and

$$\begin{aligned}\mathcal{L}V_e(t) &= 2e(t)^\top PS^{-1}\Big[(A_a - L_pC_a)e(t) \\ &\quad + L_su_s(t) - H_af(t)\Big] \\ &= e(t)^\top\Big[PS^{-1}(A_a - L_pC_a) \\ &\quad + (A_a - L_pC_a)^\top S^{-\top}P\Big]e(t) \\ &\quad + 2e(t)^\top PS^{-1}\Big[L_su_s(t) - H_af(t)\Big]. \end{aligned} \tag{26}$$

Recalling that $L_s = SP^{-1}C_a^\top U^\top = H_a$ *and* $H_aS^{-\top}P = UC_a$*, the second term of (26) becomes*

$$\begin{aligned} 2e(t)^\top PS^{-1}&\Big[L_su_s(t) - H_af(t)\Big] \\ &= 2e(t)^\top PS^{-1}H_au_s(t) - 2e(t)^\top PS^{-1}H_af(t) \\ &= 2e(t)^\top C_a^\top U^\top u_s(t) - 2e(t)^\top C_a^\top U^\top f(t) \\ &= 2\sigma_e(t)^\top u_s(t) - 2\sigma_e(t)^\top f(t) \\ &= -2\mu_o\sigma_e(t)^\top sign(\sigma_e(t)) - 2\sigma_e(t)^\top f(t) \\ &\le -2\mu_o\|\sigma_e(t)\| + 2\|\sigma_e(t)\|\|f(t)\| \\ &\le -2\big(\mu_o - (f_a^* + f_s^*)\big)\|\sigma_e(t)\|. \end{aligned} \tag{27}$$

Now, if we select $\mu_o \ge (f_a^* + f_s^* + \eta)$*, where* $\eta > 0$*, then (27) becomes*

$$2e(t)^\top PS^{-1}\Big[L_su_s(t) - H_af(t)\Big] \le -2\eta\|\sigma_e(t)\|. \tag{28}$$

Thus, from (24), (25) and (28), we have

$$\begin{aligned}
\mathcal{L}V(t) &= \mathcal{L}V_{\hat{x}}(t) + \mathcal{L}V_e(t) \\
&\leq \hat{x}(t)^\top \Big[Q(A - BK_x) + (A - BK_x)^\top Q \Big] \hat{x}(t) \\
&\quad + 2\hat{x}(t)^\top Q \Big[B(GB)^{-1}G - I \Big] L_{p_1} C_a e(t) \\
&\quad - 2\hat{x}(t)^\top QBK_r r(t) \\
&\quad + e(t)^\top \Big[PS^{-1}(A_a - L_p C_a) \\
&\quad + (A_a - L_p C_a)^\top S^{-\top} P \Big] e(t) - 2\eta \|\sigma_e(t)\| \\
&\leq \left[\hat{x}(t)^\top \ e(t)^\top \ r(t)^\top \right] \Gamma \left[\hat{x}(t)^\top \ e(t)^\top \ r(t)^\top \right]^\top .
\end{aligned} \tag{29}$$

Thus, it is evident from (29) that if the matrix constraint $\Gamma < 0$*, then* $\mathcal{L}V(t) \leq 0$*, which means that the overall closed-loop system (21) is asymptotically stable. This completes the proof.*

The condition proposed in Theorem 1 includes a linear matrix equality, which is difficult to solve directly by MATLAB toolbox. To overcome this difficulty the following algorithm is employed. The linear matrix equality (23) can be equivalently rewritten as

$$\text{trace}\Big[\left(H_a^\top S^{-\top} P - UC_a \right)^\top \left(H_a^\top S^{-\top} P - UC_a \right) \Big] = 0. \tag{30}$$

Let us introduce the following condition [23, 24]

$$\left(H_a^\top S^{-\top} P - UC_a \right)^\top \left(H_a^\top S^{-\top} P - UC_a \right) < \epsilon I_{n+p}, \tag{31}$$

where $\epsilon > 0$ is the parameter involved with the optimization problem. By Schur compliment (31) can be written as

$$\begin{bmatrix} -\epsilon I_{n+p} & \left(H_a^\top S^{-\top} P - UC_a \right)^\top \\ \star & -I_{m+p} \end{bmatrix} < 0. \tag{32}$$

Hence, the problem of solving the matrix condition (22) and (23) is converted into a problem of finding a global solution of the minimization of ϵ subject to inequalities (22) and (32). This problem is a minimization problem and can be solved by using the solvers *mincx* in the LMI toolbox of MATLAB.

3.4. Reachability Condition of Switching Surface

This section proves the guaranteed reachability condition of both the sliding surfaces $\sigma_e(t)$ defined in (15) and $\sigma_{\hat{x}}(t)$ defined in (18) in both error estimation and state estimation spaces in the following theorem.

Theorem 2. *For the observer gains L_P, L_D, and L_s designed in previous sections, and the matrices P, Q, and U are designed by satisfying the matrix constraints (22) and (32), with the discontinuous observer input $u_s(t)$ defined in (16) and discontinuous control input $u(t)$ defined in (17), the trajectories of the closed-loop system (21) in both error estimation and state estimation spaces can be kept onto the corresponding switching surfaces $\sigma_e(t)$ and $\sigma_{\hat{x}}(t)$, respectively.*

PROOF. *Choosing the Lyapunov function $V_s(t)$ as*

$$V_s(t) = V_{s_{\hat{x}}}(t) + V_{s_e}(t), \tag{33}$$

where

$$V_{s_{\hat{x}}}(t) = \frac{1}{2}\sigma_{\hat{x}}(t)^\top \sigma_{\hat{x}}(t), \tag{34}$$

and

$$V_{s_e}(t) = \frac{1}{2}\sigma_e(t)^\top \left(H_a^\top S^{-\top} P S^{-1} H_a\right)^{-1} \sigma_e(t). \tag{35}$$

Note that, the $\left(H_a^\top S^{-\top} P S^{-1} H_a\right)^{-1}$ is positive definite as H_a has full column rank. Differentiating (15) along the trajectories of (21b), we get

$$\dot{\sigma}_e(t) = H_a^\top S^{-\top} P S^{-1} \Big[(A_a - L_p C_a)e(t) + L_s u_s(t) - H_a f(t)\Big]. \tag{36}$$

Again, differentiating (35) we get

$$\begin{aligned}\dot{V}_{s_e}(t) &= \sigma_e(t)^\top \left(H_a^\top S^{-\top} P S^{-1} H_a\right)^{-1} \dot{\sigma}_e(t) \\ &= \sigma_e(t)^\top \left(H_a^\top S^{-\top} P S^{-1} H_a\right)^{-1} H_a^\top S^{-\top} P S^{-1} \\ &\quad \times \Big[(A_a - L_p C_a)e(t) + L_s u_s(t) - H_a f(t)\Big].\end{aligned} \tag{37}$$

Now, using the expression derived in Theorem 1, the last two terms of (37) can be written as

$$\begin{aligned}\sigma_e(t)^\top \left(H_a^\top S^{-\top} P S^{-1} H_a\right)^{-1} H_a^\top S^{-\top} P S^{-1} \\ \times\big[L_s u_s(t) - H_a f(t)\big] \\ = \sigma_e(t)^\top \big(u_s(t) - f(t)\big) \\ \leq -\eta \|\sigma_e(t)\|. \end{aligned} \tag{38}$$

Thus, (37) becomes

$$\begin{aligned}\dot{V}_{s_e}(t) = \sigma_e(t)^\top \left(H_a^\top S^{-\top} P S^{-1} H_a\right)^{-1} H_a^\top S^{-\top} P S^{-1} \\ \times (A_a - L_p C_a) e(t) - \eta \|\sigma_e(t)\| \\ \leq \|\sigma_e(t)\| \Big[-\eta + \| \left(H_a^\top S^{-\top} P S^{-1} H_a\right)^{-1} \| \\ \|H_a^\top S^{-\top} P S^{-1}\| \|(A_a - L_p C_a)\| \|e(t)\| \Big] \end{aligned} \tag{39}$$

Thus, for any value of

$$\begin{aligned}\eta \geq \| \left(H_a^\top S^{-\top} P S^{-1} H_a\right)^{-1} \| \|H_a^\top S^{-\top} P S^{-1}\| \\ \|(A_a - L_p C_a)\| \|e(t)\|, \end{aligned}$$

(39) is finally obtained as

$$\dot{V}_{s_e}(t) \leq 0. \tag{40}$$

Similarly, differentiating (18) along the trajectories of (12), we get

$$\begin{aligned}\dot{\sigma}_{\hat{x}}(t) = G\Big(A\hat{x}(t) - L_{p_1} C_a e(t) + Bu(t) + Bu_{s_1}(t) \\ -A\hat{x}(t) + BK_x\hat{x}(t) + BK_r r(t)\Big) \\ = -GL_{p_1} C_a e(t) + u(t) + u_{s_1}(t) \\ +K_x\hat{x}(t) + K_r r(t) \\ = -GL_{p_1} C_a e(t) - \mu_{c_1}\sigma_{\hat{x}}(t) - \mu_{c_2} sign(\sigma_{\hat{x}}(t)) \\ +u_{s_1}(t). \end{aligned} \tag{41}$$

Now, differentiating (34), we get

$$\begin{aligned}\dot{V}_{s_{\hat{x}}}(t) &= \sigma_{\hat{x}}(t)^{\top}\dot{\sigma}_{\hat{x}}(t)\\ &= \sigma_{\hat{x}}(t)^{\top}\Big[-GL_{p_1}C_a e(t) - \mu_{c_1}\sigma_{\hat{x}}(t)\\ &\quad -\mu_{c_2} sign(\sigma_{\hat{x}}(t)) + u_{s_1}(t)\Big]\\ &\leq \|GL_{p_1}C_a\|\|e(t)\|\|\sigma_{\hat{x}}(t)\| - \mu_{c_1}\sigma_{\hat{x}}(t)^2\\ &\quad -\mu_{c_2}\|\sigma_{\hat{x}}(t)\| + \sigma_{\hat{x}}(t)^{\top}u_{s_1}(t). \end{aligned} \tag{42}$$

Noticing that

$$\sigma_{\hat{x}}(t)^{\top}u_{s_1}(t) \leq (f_a^* + f_s^* + \eta)\|\sigma_{\hat{x}}(t)\|$$

Thus, (42) becomes

$$\begin{aligned}\dot{V}_{s_{\hat{x}}}(t) \leq -\mu_{c_1}\sigma_{\hat{x}}(t)^2 - \Big(&\mu_{c_2} - \|GL_{p_1}C_a\|\|e(t)\|\\ &-(f_a^* + f_s^* + \eta)\Big)\|\sigma_{\hat{x}}(t)\|. \end{aligned} \tag{43}$$

For any value of $\mu_{c_2} \geq (f_a^* + f_s^* + \eta) + \|GL_{p_1}C_a\|\|e(t)\|$*, (42) is finally obtained as*

$$\dot{V}_{s_{\hat{x}}}(t) \leq 0. \tag{44}$$

Thus, from (40) and (45), it follows that

$$\dot{V}_s(t) = \dot{V}_{s_{\hat{x}}}(t) + \dot{V}_{s_e}(t) \leq 0, \tag{45}$$

which implies that the reachability of the sliding surfaces in both state estimation and error estimation spaces can be guaranteed with the proposed controller. This completes the proof.

3.5. Design of Feedback and Feed-Forward Control Gain

The feedback control gain K_x can be designed by any state feedback control design method to achieve the desired nominal performance. In this work, K_x is designed satisfying the infinite horizon Linear Quadratic Regulator (LQR) cost function to achieve optimal control input. The LQR problem to design K_x and

K_r is stated below.

Determine the nominal control $u_c(t)$ by solving the cost function

$$J_{cf} = \min_{u_c(t)} \int_0^\infty \big(\hat{x}(\tau)^\top Q_c \hat{x}(\tau) + u_c(\tau)^\top R_c u_c(\tau)\big) d\tau \tag{46}$$

subject to

$$A\hat{x}(t) + Bu_c(t) = 0, \tag{47a}$$

$$C\hat{x}(t) = r(t), \tag{47b}$$

where $Q_c \geq 0 \in \mathbb{R}^{n\times n}$ and $R_c > 0 \in \mathbb{R}^{m\times m}$ are appropriate weighing matrices. The values of K_x and K_r to satisfy (46) and (47) are given by [25]

$$K_x = R_c^{-1} B^\top P_c \tag{48}$$

and

$$K_r = \big(C(A - BK_x)^{-1}B\big)^{-1} \tag{49}$$

where P_c is the symmetric positive definite matrix which satisfies the algebraic Riccati equation

$$A^\top P_c + P_c A + Q_c - P_c B R_c^{-1} B^\top P_c = 0. \tag{50}$$

4. Application to PWR Nuclear Power Plant

In this section, the efficacy of the proposed FE based FTC scheme discussed in Section 3 has been illustrated through simulation results by applying it to a PWR-NPP in the presence of actuator and sensor faults. The non-linear dynamic model of PWR-NPP adopted in this study considers the dynamics of the reactor core, thermal hydraulics, piping and plenum, pressurizer, steam generator, condenser, and turbine-governor system, in addition to various actuators and sensors. A detailed description of the model and its associated subsystems can be found in [26, 27, 28]. A simplified block diagram of the PWR-NPP showing interconnections of various subsystems is shown in Fig. 1. First, the nonlinear model of PWR-NPP is linearised around the steady state operating

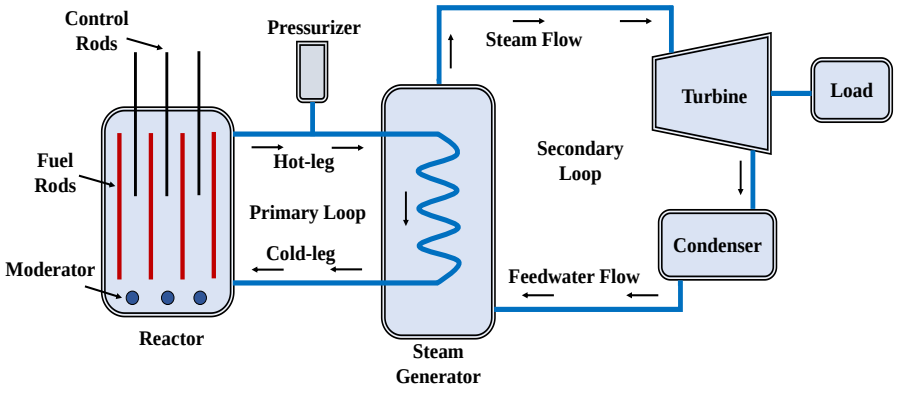

Figure 1: A simple block diagram representation of different interconnected subsystems in a PWR-NPP.

point to obtain the linear model, which is then used to design the proposed FE based FTC scheme. For definitions of the system state vector $x(t)$, the control input vector $u(t)$, the output vector $y(t)$, and the elements of the system matrices A, B, and C, for each control loop the readers are kindly referred to [29]. The proposed FTC scheme is designed to achieve stable response as well as adequate degree of robustness in the presence of faults. In this study, the proposed control algorithm is applied to reactor core power control loop and steam generator pressure control loop of the PWR-NPP and its performance is tested in the presence of both actuator and sensor faults for set-point change. However, the proposed control scheme can be designed and successfully applied to other control loops of PWR-NPP, such as temperature control loop, pressurizer pressure and level control loop, and turbine speed control loop.

4.1. Reactor Power Control Loop (Load Following Mode of Operation)

In load-following mode of operation, the reactor power adjusts according to the electricity demand throughout the day. The reactor power is controlled by varying the control rod movement speed $v_{rod}(t)$ and the reactor power is measured with the help of excore detector current $i_{lo}(t)$. For this control loop, the values of design parameters for the FE proposed in (4) and the FTC proposed

in (17) are selected as follows: The matrix L_D is selected as $[0_{24\times 1}\ 1]^\top$, the discontinuous observer gain μ_o is selected as 0.2, and the matrix $P \in \mathbb{R}^{25\times 25}$ is obtained with help of LMI Toolbox of MATLAB. The state feedback control gain K_x is designed with help of LQR control technique by selecting the values of Q_c and R_c as $1\times 10^{-3} I_{25}$ and 1×10^{3}, respectively. The discontinuous control gains μ_{c_1} and μ_{c_2} are selected as 0.1 and 1, respectively.

Here, the objective is to track the demand power variations precisely in spite of the presence of actuator and sensor faults in the system. It is assumed that the actuator fault $f_a(t)$ and sensor fault $f_s(t)$ have the following form

$$f_a(t) = \Big\{ 5\times 10^{-4}\ \sin(0.1t),\ t > 0$$

$$f_s(t) = \begin{cases} 5\times 10^{-3} + 1\times 10^{-2}\ \sin(0.2(t-1)),\ t > 250 \\ 0, \qquad\qquad\qquad\qquad \text{elsewhere.} \end{cases}$$

To cover a wide variety of time varying faults, we have considered the above mentioned faults in the system. In the literature [23, 24], sinusoidal type of faults are considered to test the effectiveness of controllers and the similar type has been adopted here. The reference excore detector current corresponds to demand power is varied as follows:

$$i_{lo}^{ref}(t) = \begin{cases} 19.6554, & 0 \le t \le 100 \\ 19.6554 - 4.5\times 10^{-3}(t-100), & 100 < t \le 120 \\ 19.5658, & \text{elsewhere.} \end{cases}$$

First, the performance of the robust observer is analysed. As the actuator fault will be automatically overcome by the SMC, in this study, only the sensor fault has been estimated and the information of which is then used to design the FTC. Initially, it is assumed that the reactor is operating at steady state and all the state variables are in equilibrium. The initial condition for the estimated states are considered same as that of the actual states and for the estimated fault it is considered equal to zero. Fig. 2 shows the variation of actual sensor fault and estimated sensor fault with the robust FE as proposed in (4). It can be observed that the proposed estimator is able to estimate the sensor fault

perfectly in spite of the presence of actuator fault in the system. To show the robustness of the proposed estimator over conventional observer, the proposed estimator performance is compared with the PI observer (setting the discontinuous injection input $u_s(t) = 0$ in (4)). From Fig. 3, it can be observed that, the PI observer is unable to follow the sensor fault and the observer performance is badly affected by the actuator fault present in the system.

Secondly, the performance of the overall FE based FTC scheme is analysed. The response of the closed-loop system with and without FTC scheme is shown in Fig. 4. It can be observed that the proposed FTC scheme is able to overcome both actuator as well as sensor fault present in the system while, without FTC scheme, the system performance is badly affected by the faults. As the actuator fault satisfies the matching condition, its effect is automatically overcome by the SMC while, to eliminate the effect caused by the sensor fault, the output of the system is compensated by the estimated sensor fault. Furthermore, the closed-loop system response in fault free condition is also analysed and it is shown in Fig. 5. It can be observed that the performance of the proposed FTC is almost identical to the performance in fault free condition. During transient variation of control rod speed movement is shown in Fig. 6. Control input can be observed to be free from chattering. To cancel the effect of sinusoidal actuator fault, control rod movement speed is also varying sinusoidally but the magnitude of oscillation is very less.

4.2. Steam Generator Pressure Control Loop

In this control loop, objective is to maintain the pressure in the steam generator. The steam generator pressure $P_s(t)$ is controlled by adjusting the input signal to the turbine-governor valve $u_{tg}(t)$. For this control loop, the values of design parameters for the FE proposed in (4) and the FTC proposed in (17) are selected as follows:

- $L_D = [0_{24\times 1}\ 1]^\top$
- $\mu_o = 5$

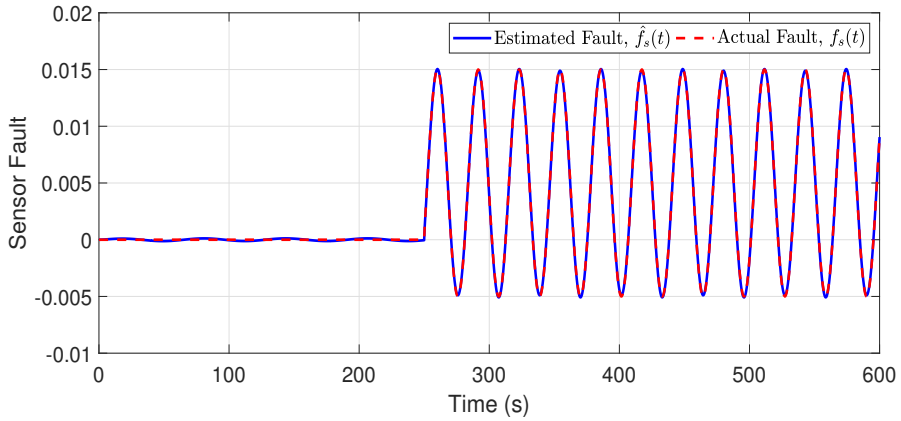

Figure 2: Actual and estimated sensor fault with discontinuous injection.

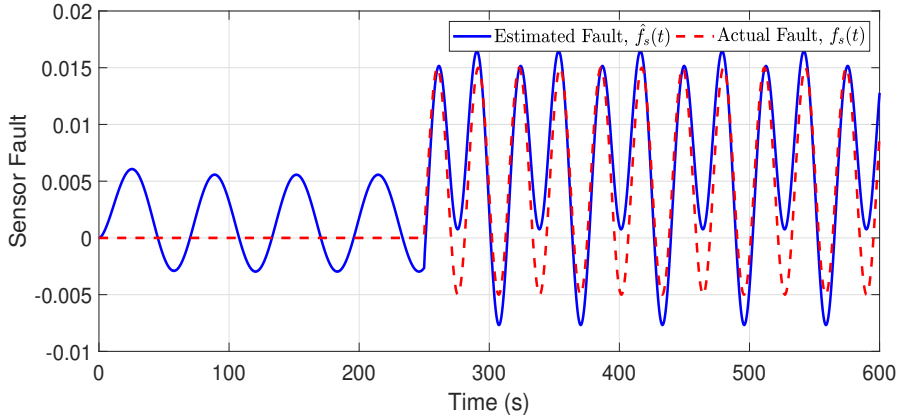

Figure 3: Actual and estimated sensor fault without discontinuous injection.

- $Q_c = 0.1I_{25}$ and $R_c = 1 \times 10^3$
- $\mu_{c_1} = 10$ and $\mu_{c_2} = 1$.

It is assumed that the actuator fault $f_a(t)$ and sensor fault $f_s(t)$ have the following form

$$f_a(t) = \begin{cases} 6 \times 10^{-3} \sin(0.1t), t > 0 \end{cases}$$

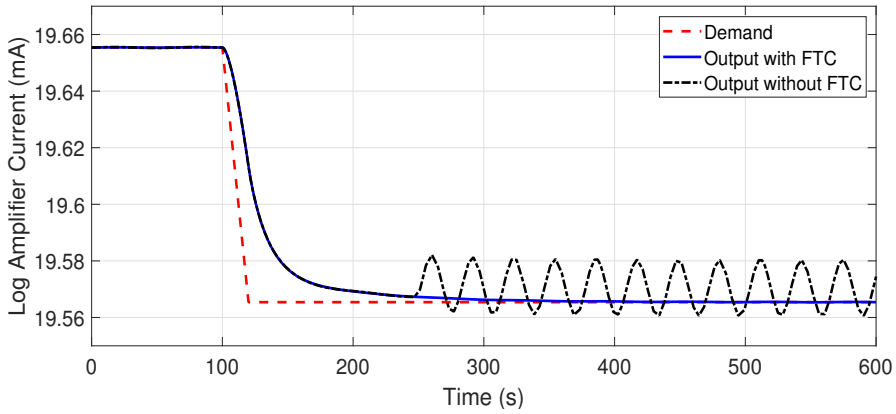

Figure 4: Excore detector current with and without fault tolerant control.

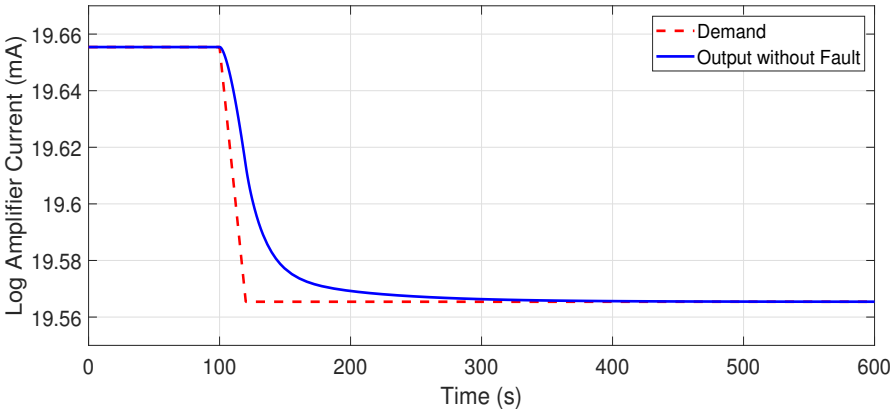

Figure 5: Excore detector current in fault free condition.

$$f_s(t) = \begin{cases} 1 \times 10^{-3} + 3 \times 10^{-3} \\ \quad \times \sin(0.15(t-1)), & 200 \geq t < 350 \\ 5 \times 10^{-3} \sin(0.3t + \pi), & 350 \geq t < 500 \\ 0, & \text{elsewhere} \end{cases}$$

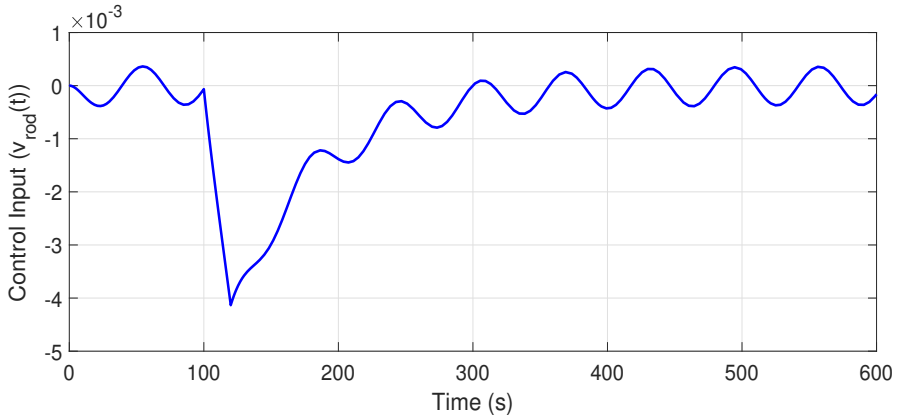

Figure 6: Control rod speed moment during demand power manoeuvring.

The reference signal change in secondary pressure is applied as follows:

$$p_s^{ref} = \begin{cases} 7.29, & 0 \leq t \leq 50 \\ 8.86 \times 10^{-4}(t-50) + 7.29, & 50 < t \leq 100 \\ 7.33, & 100 < t \leq 300 \\ -8.86 \times 10^{-4}(t-300) + 7.33, & 300 < t \leq 350 \\ 7.29, & \text{elsewhere.} \end{cases}$$

Similar to reactor core power control loop, in this loop also first performance of the proposed FE is analysed. Figs. 7 and 8 show the variation of actual sensor fault and estimated sensor fault for the proposed FE and PI observer, respectively. In this case also, it can be observed that, compared to PI observer the proposed estimator able to estimate the sensor fault perfectly in spite of the presence of actuator fault in the system. Secondly, the performance of the overall FE based FTC scheme is analysed. The response of the closed-loop system with and without FTC scheme is shown in Fig. 9. It can be observed that the proposed FTC scheme is able to overcome both actuator as well as sensor fault more effectively compared the closed-loop system without FTC scheme. The closed-loop system response in fault free condition is shown in Fig. 10. In this case also, it can be observed that the performance of the proposed FTC is almost identical to the performance in fault free condition. Finally,

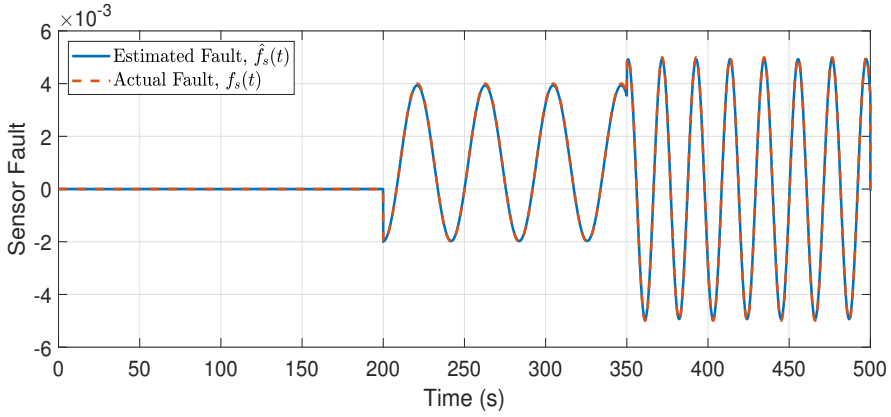

Figure 7: Actual and estimated sensor fault with discontinuous injection.

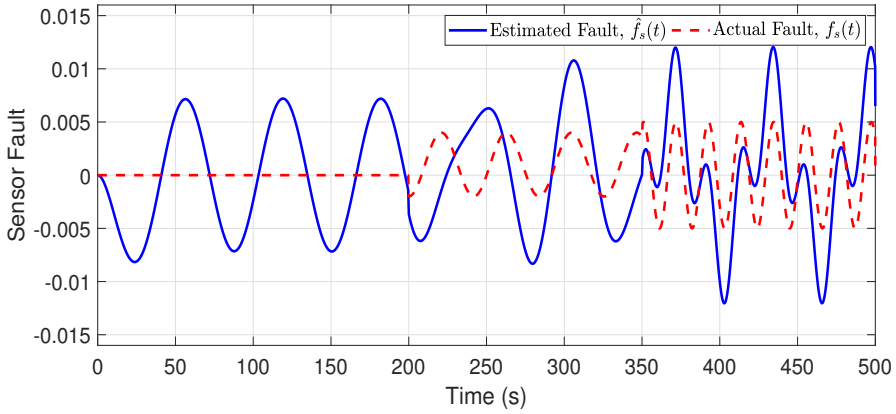

Figure 8: Actual and estimated sensor fault without discontinuous injection.

variation of control signal to turbine-governor valve is shown in Fig. 11.

5. Conclusions

In this paper, the problem of simultaneous state and fault estimation and fault-tolerant controller design has been investigated for pressurized water reactor type nuclear power plant subject to simultaneous actuator and sensor faults. A descriptor sliding mode observer has been proposed to obtain the estimates for both system states and sensor faults simultaneously. Based on the

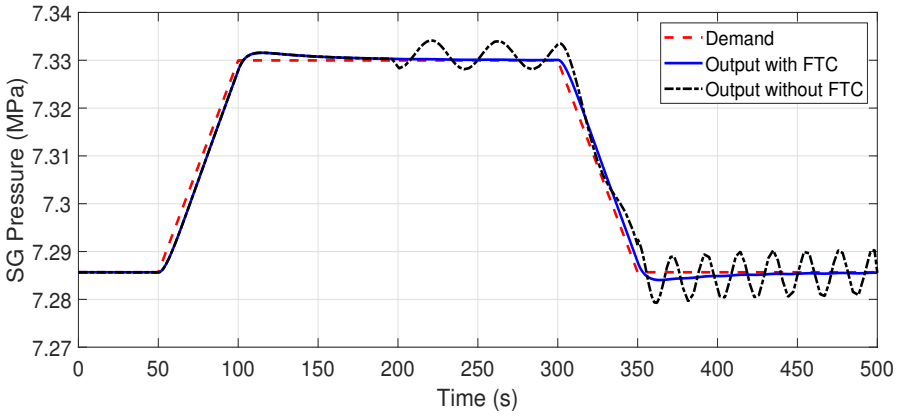

Figure 9: Steam generator pressure with and without fault tolerant control.

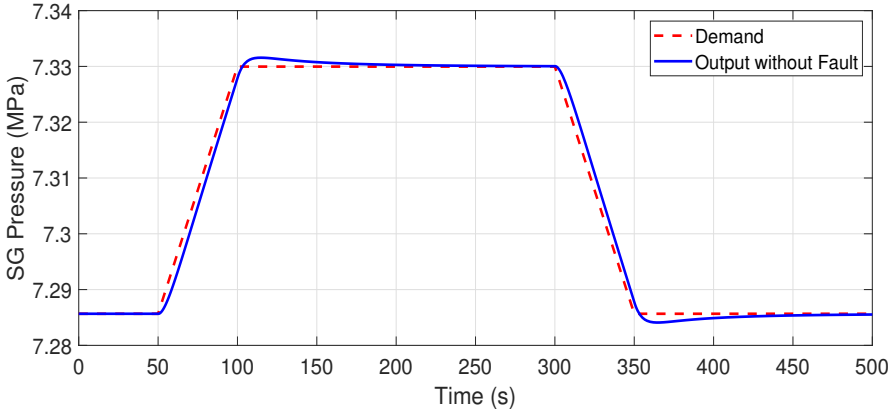

Figure 10: Steam generator secondary pressure in fault free condition.

information provided by the observer, a fault tolerant controller is designed using integral sliding mode control technique to stabilize the resulting closed-loop system. A sufficient condition based on the feasibilities of linear matrix inequalities is derived for the asymptotic stability of the overall closed-loop system. Finally, the effectiveness of the proposed fault tolerant control scheme has been demonstrated by applying it to reactor power control loop and steam generator pressure control loop of pressurized water reactor type nuclear power plant. Future work will consider apply the proposed fault tolerant control technique

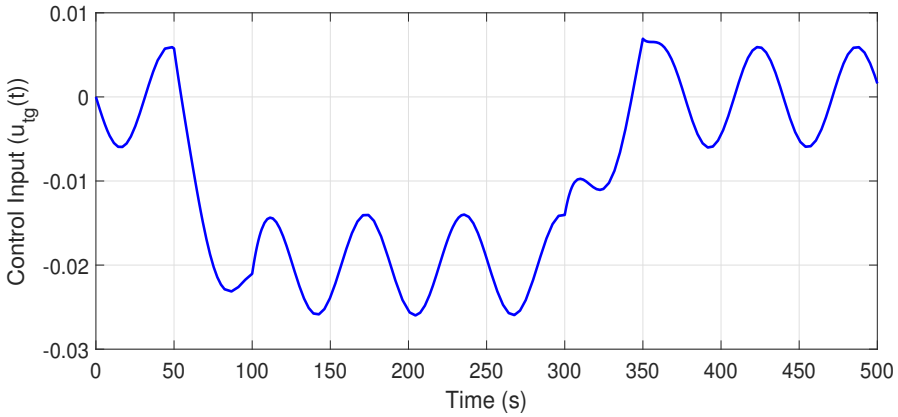

Figure 11: Control signal to turbine-governor valve.

to faulty systems considering different types and combinations of the faults and measurement noise.

Acknowledgement

This research was funded by the Engineering and Physical Sciences Research Council (EPSRC) grant number EP/R021961/1.

A. Proof of Lemma 1

PROOF. It is observed that the system matrices E_a and C_a satisfy

$$\text{rank}\begin{bmatrix} E_a \\ C_a \end{bmatrix} = \text{rank}\left[\begin{array}{c|c} I_n & 0_{n\times p} \\ 0_{p\times n} & 0_{p\times p} \\ \hline C & I_p \end{array}\right] = n + p. \tag{51}$$

Let us define L_D as

$$L_D = \begin{bmatrix} 0_{n\times p} \\ W \end{bmatrix},$$

where $W \in \mathbb{R}^{p\times p}$ and is selected as $W = \text{diag}(w_1,\ w_2,\ \ldots,\ w_p)$ with $w_i > 0$. Thus,

$$S = (E_a + L_D C_a) = \begin{bmatrix} I_n & 0_{n\times p} \\ WC & W \end{bmatrix},$$

$$S^{-1} = \begin{bmatrix} I_n & 0_{n\times p} \\ -C & W^{-1} \end{bmatrix},$$

$$C_a S^{-1} L_D = \begin{bmatrix} C & I_p \end{bmatrix} \begin{bmatrix} I_n & 0_{n\times p} \\ WC & W \end{bmatrix} \begin{bmatrix} 0_{n\times p} \\ W \end{bmatrix} = I_p,$$

and

$$\begin{aligned} A_a S^{-1} L_D &= \begin{bmatrix} A & 0_{n\times p} \\ 0_{p\times n} & -I_p \end{bmatrix} \begin{bmatrix} I_n & 0_{n\times p} \\ WC & W \end{bmatrix} \begin{bmatrix} 0_{n\times p} \\ W \end{bmatrix} \\ &= \begin{bmatrix} 0_{n\times p} \\ -I_p \end{bmatrix} = -R. \end{aligned}$$

This completes the proof.

References

[1] V. Vajpayee, V. Becerra, N. Bausch, S. Banerjee, J. Deng, S. R. Shimjith, A. John Arul, Robust subspace predictive control based on integral sliding mode for a pressurized water reactor, in: 2020 7th International Conference on Control, Decision and Information Technologies (CoDIT), Vol. 1, 2020, pp. 7–12.

[2] R. J. Desai, B. M. Patre, R. K. Munje, A. P. Tiwari, S. R. Shimjith, Integral sliding mode for power distribution control of advanced heavy water reactor, IEEE Transactions on Nuclear Science 67 (6) (2020) 1076–1085.

[3] B. M. Patre, P. S. Londhe, R. M. Nagarale, Fuzzy sliding mode control for spatial control of large nuclear reactor, IEEE Transactions on Nuclear Science 62 (5) (2015) 2255–2265.

[4] N. Zare Davijani, G. Jahanfarnia, A. Esmaeili Abharian, Nonlinear fractional sliding mode controller based on reduced order FNPK model for output power control of nuclear research reactors, IEEE Transactions on Nuclear Science 64 (1) (2017) 713–723.

[5] K. K. Abdulraheem, S. A. Korolev, Robust optimal-integral sliding mode control for a pressurized water nuclear reactor in load following mode of operation, Annals of Nuclear Energy 158 (2021) 108288.

[6] S. Mostafavi, G. Ansarifar, Pressurizer water level control with estimation of primary circuit coolant mass in nuclear power plants via robust observer based dynamic sliding mode control, Annals of Nuclear Energy 161 (2021) 108413.

[7] C. Edwards, S. K. Spurgeon, Sliding Mode Control: Theory and Applications, Taylor and Francis, 1998.

[8] S. Gautam, P. K. Tamboli, V. H. Patankar, K. Roy, S. P. Duttagupta, Sensors incipient fault detection and isolation using kalman filter and kullback–leibler divergence, IEEE Transactions on Nuclear Science 66 (5) (2019) 782–794.

[9] S. Gautam, P. K. Tamboli, K. Roy, V. H. Patankar, S. P. Duttagupta, Sensors incipient fault detection and isolation of nuclear power plant using extended kalman filter and Kullback–Leibler divergence, ISA Transactions 92 (2019) 180–190.

[10] V. Yellapu, A. Tiwari, S. Degweker, Application of data reconciliation and fault detection and isolation of ion chambers in advanced heavy water reactor, Annals of Nuclear Energy 85 (2015) 1210–1225.

[11] V. S. Yellapu, V. Vajpayee, A. P. Tiwari, Online fault detection and isolation in advanced heavy water reactor using multiscale principal component analysis, IEEE Transactions on Nuclear Science 66 (7) (2019) 1790–1803.

[12] V. S. Yellapu, W. Zhang, V. Vajpayee, X. Xu, A multiscale data reconciliation approach for sensor fault detection, Progress in Nuclear Energy 135 (2021) 103707.

[13] E. Hatami, H. Salarieh, N. Vosoughi, Design of a fault tolerated intelligent control system for a nuclear reactor power control: Using extended kalman filter, Journal of Process Control 24 (7) (2014) 1076–1084.

[14] E. Hatami, N. Vosoughi, H. Salarieh, Design of a fault tolerated intelligent control system for load following operation in a nuclear power plant, International Journal of Electrical Power and Energy Systems 78 (2016) 864–872.

[15] N. Khentout, H. Salhi, Giovanni Magrotti, D. Merrouche, Fault monitoring and accommodation of the heat exchanger parameters of triga-mark ii nuclear research reactor using model-based analytical redundancy, Progress in Nuclear Energy 109 (2018) 97–112.

[16] P. H. Rangegowda, S. C. Patwardhan, S. Mukhopadhyay, Fault tolerant control of a nuclear steam generator in the presence of sensor biases, IFAC-PapersOnLine 53 (1) (2020) 579–584, 6th Conference on Advances in Control and Optimization of Dynamical Systems ACODS 2020.

[17] P. Wang, Q. Jiang, J. Zhang, J. Wan, S. Wu, A fuzzy fault accommodation method for nuclear power plants under actuator stuck faults, Annals of Nuclear Energy 165 (2022) 108674.

[18] G. Ablay, T. Aldemir, Fault detection in nuclear systems using sliding mode observers, Nuclear Science and Engineering 173 (1) (2013) 82–98.

[19] Z. Dong, Boolean network-based sensor selection with application to the fault diagnosis of a nuclear plant, Energies 10 (12).

[20] A. Evsukoff, S. Gentil, Recurrent neuro-fuzzy system for fault detection and isolation in nuclear reactors, Advanced Engineering Informatics 19 (1) (2005) 55–66.

[21] A. AItouche, B. O. Bouamama, Fault tolerant control with respect to actuator failures application to steam generator process, Computer Aided Chemical Engineering 20 (2005) 1471–1476.

[22] Y. Yu, M. jun Peng, H. Wang, Z. guo Ma, W. Li, Improved PCA model for multiple fault detection, isolation and reconstruction of sensors in nuclear power plant, Annals of Nuclear Energy 148 (2020) 107662.

[23] M. Liu, P. Shi, Sensor fault estimation and tolerant control for itô stochastic systems with a descriptor sliding mode approach, Automatica 49 (5) (2013) 1242–1250.

[24] Y. Niu, J. Lam, X. Wang, D. W. C. Ho, Observer-based sliding mode control for nonlinear state-delayed systems, International Journal of Systems Science 35 (2) (2004) 139–150.

[25] D. S. Naidu, Optimal Control Systems, CRC Press, Inc., Boca Raton, FL, USA, 2002.

[26] V. Vajpayee, V. Becerra, N. Bausch, J. Deng, S. Shimjith, A. J. Arul, Dynamic modelling, simulation, and control design of a pressurized water-type nuclear power plant, Nuclear Engineering and Design 370 (2020) 110901.

[27] V. Vajpayee, E. Top, V. M. Becerra, Analysis of transient interactions between a pwr nuclear power plant and a faulted electricity grid, Energies 14 (6).

[28] P. V. Surjagade, J. Deng, V. Vajpayee, V. M. Becerra, S. Shimjith, A. J. Arul, An arbitrary-order continuous sliding mode control technique for nonlinear pwr-type nuclear power plants, Progress in Nuclear Energy 150 (2022) 104309.

[29] V. Vajpayee, V. Becerra, N. Bausch, J. Deng, S. R. Shimjith, A. J. Arul, L_1-adaptive robust control design for a pressurized water-type nuclear power plant, IEEE Transactions on Nuclear Science 68 (7) (2021) 1381–1398.